

## First results from the Radio Plasma Imager on IMAGE

B. W. Reinisch<sup>1</sup>, X. Huang<sup>1</sup>, D. M. Haines<sup>1</sup>, I. A. Galkin<sup>1</sup>, J. L. Green<sup>2</sup>, R. F. Benson<sup>2</sup>, S. F. Fung<sup>2</sup>, W. W. L. Taylor<sup>3</sup>, P. H. Reiff<sup>4</sup>, D. L. Gallagher<sup>5</sup>, J.-L. Bougeret<sup>6</sup>, R. Manning<sup>6</sup>, D. L. Carpenter<sup>7</sup> and S. A. Boardsen<sup>8</sup>

**Abstract.** The Radio Plasma Imager (RPI) is a 3 kHz to 3 MHz radio sounder, incorporating modern digital processing techniques and long electronically-tuned antennas, that is flown to large radial distances into the high-latitude magnetosphere on the Imager for Magnetopause-to-Aurora Global Exploration (IMAGE) satellite. Clear echoes, similar to those observed by ionospheric topside sounders, are routinely observed from the polar-cap ionosphere by RPI even when IMAGE is located at geocentric distances up to approximately 5 Earth radii. Using an inversion technique, these echoes have been used to determine electron-density distributions from the polar-cap ionosphere to the location of the IMAGE satellite. Typical echoes from the plasmopause boundary, observed from outside the plasmasphere, are of a diffuse nature indicating persistently irregular structure. Echoes attributed to the cusp and the magnetopause have also been identified, those from the cusp have been identified more often and with greater confidence.

### Introduction

The Radio Plasma Imager (RPI) on the Imager for Magnetopause to Aurora Global Exploration (IMAGE) satellite is a highly flexible, multi-mode instrument in which sounding and listening frequencies, range detection, pulse characteristics and repetition rate, are adjustable parameters over a wide range of values. The flexibility in programming the RPI allows the instrument to remotely sound magnetospheric boundaries, perform local relaxation sounding, and observe natural emissions over a selectable duty cycle. The instrument covers the frequency range from 3 kHz to 3 MHz with a receiver bandwidth of 300 Hz. There are three orthogonal thin-wire antennas, two 500-m tip-to-tip dipoles in the spin plane (X and Y), and a 20-m tip-to-tip dipole along the spin axis (Z). All three antennas are used for reception, allowing the measurement of the angle of arrival of the signals. The long dipoles, which are also used for transmission, are electronically tuned to optimize the transmis-

sion efficiency. Under conditions of free space propagation, the radiated RF power increases from ~0.1 mW at low frequencies to ~10 W per dipole at 200 kHz and above [Reinisch *et al.*, 2000]. Unfortunately, due to a single event latch-up after about one month of operation, the power supply for the Y transmitter malfunctioned on May 8, reducing the total radiated power by 3 dB.

A number of different waveforms can be selected to adapt to sounding diverse environments: a simple 3.2 ms pulse modulation with constant repetition rate; a phase-coded pulse consisting of 4, 8, or 16 of the 3.2 ms chips; a chirp pulse; and a randomly spaced sequence of 3.2 ms pulses. Selective application of pulse compression and Fourier integration processing enhances the signal-to-noise ratio nominally by 15 dB. Reinisch *et al.* [2000] have given a detailed description of the RPI.

IMAGE was launched on March 25, 2000, into a highly elliptical polar orbit with an initial apogee geocentric radial distance of 8.22 Earth radii ( $R_E$ ) on the dayside near the noon meridian [Burch, 2000]. The RPI transmissions have not caused any interference problems in the optical and neutral atom imagers on the spacecraft.

### Echoes from the High Altitude and High Latitude Magnetosphere

The primary presentation of RPI sounding data is in the form of plasmagrams, which are the magnetospheric analogs of ionograms. Figure 1 is a plasmagram that presents echo amplitudes as function of echo time delay ( $t$ ), expressed in terms of virtual range (left scale), and sounder frequency (bottom scale). It shows a trace of extraordinary (X)-mode echoes extending from ~50 kHz to 300 kHz, and local plasma resonances around 30 kHz. To enhance the signal appearance on the plasmagram the data were thresholded using a dynamic most-probable-amplitude algorithm. The virtual echo range from the spacecraft to the reflecting plasma equals  $ct/2$  where  $c$  is the free space speed of light. The intensity is color-coded in instrument units. At the time of this plasmagram IMAGE was outbound at approximately  $3.6 R_E$ , and outside the plasmopause. This plasmagram is typical of those obtained over the northern polar cap.

The electron-density ( $N_e$ ) profiles are deduced from the echoes using a numerical inversion technique that is a variation of that developed by Huang and Reinisch [1982] for the topside ionosphere. When the apparent ranges  $R'(f_k)$  are known for a set of wave frequencies  $f_k$  the inversion determines  $N_e(R)$  using the following integral equation:

$$R'(f_k) = \int_0^{R_{rk}} \mu' \left[ N_e(R), f_k, f_g(R), \theta(R) \right] dR \quad (1)$$

where:  $\mu'$  is the group index of refraction, is a function of  $N_e$ ,  $f_k$ ,  $f_g$  (which is proportional to the magnetic field strength), the ray wave normal angle  $\theta$ , and  $R_{rk}$  is the geometric distance from the spacecraft to the reflection point at the wave frequency  $f_k$ . Since the echoes are propagating in a free-space mode, they are either in the left-hand ordinary (L-O) or right-hand extraordinary (R-X) mode. Using a magnetic-field model and the measured plasma resonances (see below) the polarization of the echo traces can be uniquely determined through an iterative process, and the density distribution can be calculated.

The resulting  $N_e(R)$  profile deduced from the plasmagram of Figure 1, and the similarly determined profiles from the previous two plasmagrams taken 8 and 16 minutes earlier, are shown in

<sup>1</sup>Center for Atmospheric Research, University of Massachusetts, Lowell

<sup>2</sup>NASA Goddard Space Flight Center, Greenbelt, MD

<sup>3</sup>Raytheon ITSS Corporation at NASA Goddard Space Flight Center, Greenbelt, MD

<sup>4</sup>Rice University, Houston, TX

<sup>5</sup>NASA Marshall Space Flight Center, Huntsville, AL

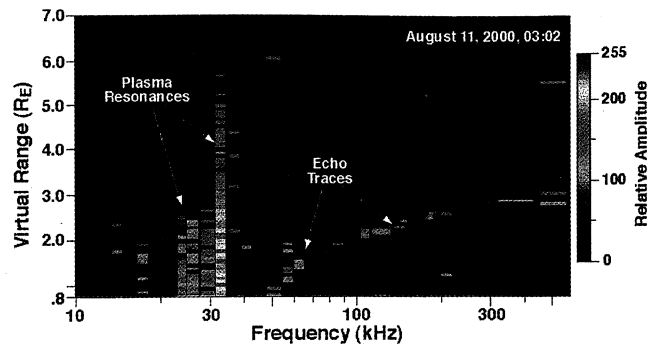
<sup>6</sup>Observatoire de Paris, Meudon, France

<sup>7</sup>STAR Laboratory, Stanford University, Stanford, CA

<sup>8</sup>Emergent Information Technologies, Inc. at NASA Goddard Space Flight Center, Greenbelt, MD

Copyright 2001 by the American Geophysical Union.

Paper number 2000GL012398.  
0094-8276/01/2000GL012398\$05.00



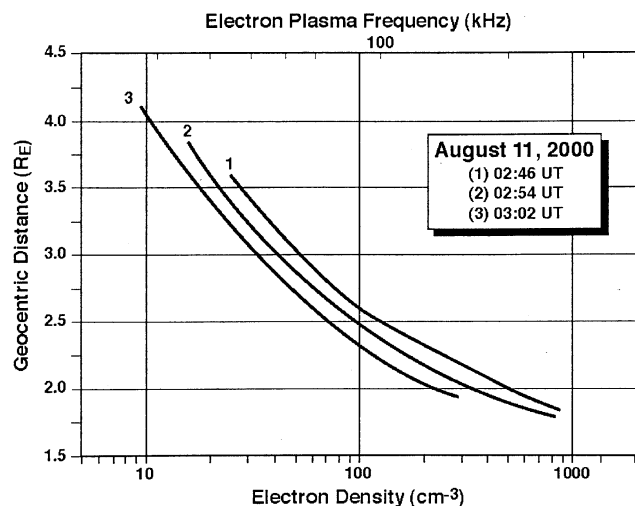
**Figure 1.** RPI plasmagram with polar cap echoes from approximately 50 to 300 kHz starting at 03:02 UT on August 11, 2000, (13:6 MLT) showing echo amplitudes as a function of frequency and virtual range. A number of local resonances are also detected around 30 kHz. The plasmagram duration is approximately one minute.

Figure 2. The electron plasma frequency ( $f_p$ ), plotted on the top axis, is related to  $N_e$  on the bottom axis by the expression  $f_p^2(\text{kHz}) \approx 80.6 N_e (\text{cm}^{-3})$ . As shown in Figure 2,  $N_e$  extends from  $10\text{--}25 \text{ cm}^{-3}$  at the spacecraft and to  $\sim 900 \text{ cm}^{-3}$  in the topside polar-cap ionosphere. Although the RPI direction-finding technique [Reinisch *et al.*, 1999] has not been fully implemented, there is sufficient indication that the echoes in these plasmagrams resulted from radio waves propagating from the direction of the northern polar cap.

RPI has also observed echoes from the cusp and the magnetopause that are generally weak and diffuse, especially those from the magnetopause [Fung *et al.*, 2000a]. The echoes from the polar cusp do provide an indication of the prevailing  $N_e$  structure in the cusp [Henize *et al.*, 2000].

### Echoes Near the Plasmasphere

Figure 3 shows a typical plasmagram observed near, but beyond, the plasmapause. From a combination of preliminary direction finding measurements, comparison with ray tracing simulations [see for example Green *et al.*, 2000], and



**Figure 2.** The polar cap electron density profiles calculated from successive plasmagrams on August 11, 2000. IMAGE was outbound, well outside the plasmapause, over the polar cap. As expected, the local  $N_e$  decreases steadily, as does the entire profile, when approaching the central cap.

expectations based on passive density measurements from IMAGE itself (illustrated for another orbit below), it is clear that the discrete echoes, labeled in Figure 3, are not coming directly from the plasmapause but result from radio waves following field-aligned  $N_e$  irregularities or ducts. Such propagation paths from satellite-borne sounders have been well documented in the ionosphere [Muldrew, 1963] and have been proposed for magnetospheric research [Calvert, 1981].

Ray tracing calculations [see Green *et al.*, 2000] and simple geometric considerations suggest that RPI should observe discrete, direct echo traces reflected from the plasmapause but those types of echoes are only rarely observed. Instead, as shown in Figure 3, diffuse echoes are observed. These diffuse echoes may be similar in nature to the spread F phenomenon observed in ionospheric topside sounder data [James, 1989]. Various forms of satellite and ground data, as well as theory, suggest that the plasmasphere "surface" can be irregular over a wide range of scale lengths [see, e.g., Oya and Ono, 1987; Carpenter and Lemaire, 1997]. Since RPI will be probing the plasmasphere boundary at various latitudes and local times it is anticipated that new insights into the origin and properties of these irregularities will be obtained [Fung *et al.*, 2000b].

### Plasma Resonances

The RPI can also make reliable *in situ* measurements by detecting short-range electrostatic-wave echoes [e.g., see Benson, 1977 and Etcheto *et al.*, 1983] at the various resonant frequencies of a plasma. These sounder-stimulated resonances provide a means to determine the local  $f_p$  and  $f_g$  which are important parameters in the profile inversion process.

Although plasma resonances are often detected in the plasmagrams of the type shown in Figures 1 and 3, higher accuracy and resolution is achieved when RPI is programmed to transmit short (3.2 ms) pulses, with a constant difference between frequency transmissions comparable to the RPI receiver bandwidth of 300 Hz. Local resonances have been stimulated before by magnetospheric radio sounders, but never at such great radial distances at high latitudes. Even at the high-latitude IMAGE apogee, resonances up to  $18 f_g$  have been observed and the time duration of the lower-order harmonics can exceed 100 ms.

Plasma resonances at the upper-hybrid frequency  $f_{uh}$ , where  $f_{uh}^2 = f_p^2 + f_g^2$ , are also stimulated by RPI. The observed  $n f_g$ ,  $f_p$ , and  $f_{uh}$  resonances, and the wave-cutoff values, are used to self-consistently calculate the best  $f_g$  and  $f_p$  value for a given plasmagram. This method of determining  $N_e$  from plasma resonances is one of the most precise methods since it is unaffected by spacecraft charging or the partial measurement of the plasma

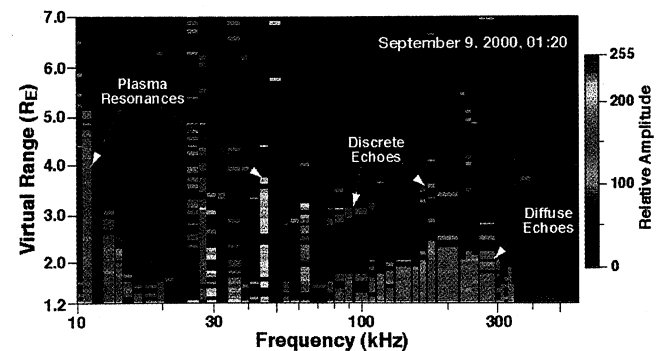


**Figure 3.** RPI plasmagram from 01:20 UT on September 9, 2000, when IMAGE was outside the plasmasphere, approximately  $1 R_E$  from the plasmapause. Both discrete and diffuse echoes are observed, in addition to local plasma resonances. The discrete echoes propagate along field-aligned ducts, while the diffuse echoes are from the plasmapause itself, indicating the presence of irregular structure.

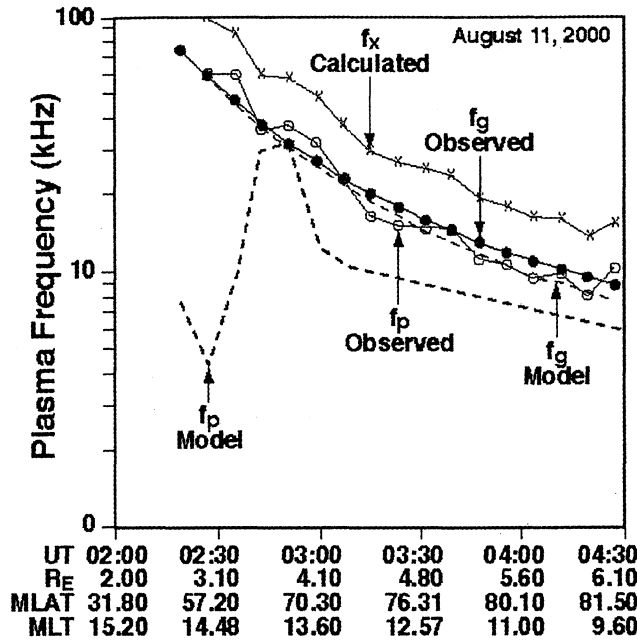


Figure 4. Comparisons between resonance-determined and model  $f_p$  and  $f_g$  values for a period of August 11, 2000 that includes the times corresponding to Figures 1 & 3.

particle distribution. The results are compared to existing models (Chappell et al. [1970] for the outer plasmasphere, Eastman et al. [2000] for the polar cusp, and Persoon et al. [1983] for the polar cap), are shown in Figure 4 for a significant portion of the August 11, 2000, IMAGE orbit. Also shown are the X-mode wave cutoff values ( $f_x$ ) that were calculated from the resonance-determined  $f_p$  and  $f_g$  values. These data are from an outbound pass starting beyond  $2 R_E$  and extending well into the polar cap at  $6.2 R_E$ .

### Passive Observations

Passive observations are typically interspersed with the sounding modes. A complete spectrum of passive measurements is generated at least once every eight minutes and sometimes every two or four minutes. These observations are used to provide a familiar context for the RPI echo observations and deduce the characteristic cutoff frequencies in the local plasma. As in the sounding mode, the electric field intensity is simultaneously measured at each of the dipole antennas with three separate receivers.

A typical RPI dynamic spectrogram from 3 kHz to 3 MHz is presented in Figure 5. Due to the long antennas and very sensitive receivers, RPI's passive measurements provides a unique set of wave observations. The green trace overlaying the spectrogram in Figure 5 is the local  $f_g$  model value. Since IMAGE's orbital period is 14.25 hours,  $f_g$  can be seen to go through nearly two complete cycles in 24 hours. The spectrogram in Figure 5 shows a number of Type III radio bursts, auroral kilometric radiation (AKR), auroral myriametric radiation (AMR) and the non-thermal continuum emissions. IMAGE's orbit is such that its apogee is on the day side at about 7 hours magnetic local time (MLT) at about  $45^\circ$  magnetic latitude on this day. It is in this region that IMAGE is in the primary emission cone of continuum radiation as determined by Morgan and Gurnett [1991], and Green and Boardsen [1999]. The few observations of AKR during these first several months of IMAGE's orbit are also consistent with the AKR observed emission cone characteristics as determined by Green et al. [1977] and Gallagher and Gurnett [1979].

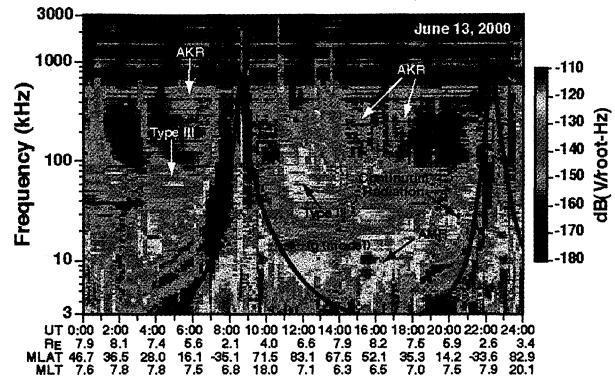


Figure 5. Frequency-time dynamic spectrogram of RPI passive measurements from the x-axis dipole during June 13, 2000. The green trace is the expected *in situ* gyrofrequency obtained from a model magnetic field. Various types of natural radio emissions are identified.

### Conclusions

Discrete echoes from the high-latitude polar cap have been used to obtain the  $N_e$  distribution over a distance of some  $2 R_E$  from the spacecraft. RPI observations from outside the plasmasphere indicate that field-aligned ducts readily exist for distances up to several  $R_E$  in this region. The diffuse echoes from the plasmopause testify to its irregular structure.

The RPI-stimulated plasma resonances permit the accurate determination of the local  $N_e$  and magnetic field magnitude at the spacecraft at radial distances never before obtained. These local measurements aid the inversion of the sounder-reflection traces into  $N_e$  profiles.

Passive operations yield dynamic spectra of natural magnetospheric emissions down to 3 kHz. These spectra help to eliminate possible confusion about the reception of echoes from active RPI transmissions, and place the sounder echo measurements into a familiar geophysical context.

These types of observations are providing precise measurements of the plasma characteristics within the Earth's magnetosphere in order to improve our understanding of the structure of the magnetosphere under a variety of magnetospheric conditions.

**Acknowledgments.** The work at University of Massachusetts Lowell, Rice University, and at Raytheon ITSS were supported by NASA under subcontracts from Southwest Research Institute. The authors thank Mark Tapley of SwRI, Rick Burley at the SMOC at GSFC, and Steve Stelmash of UML for their tireless effort in uploading new RPI measurement programs to the spacecraft.

### References

Benson, R. F., Stimulated plasma waves in the ionosphere, *Radio Sci.*, **12**, 861-878, 1977.  
 Burch, IMAGE Mission overview, *Space Sciences Review*, IMAGE special issue, **91**, 1-14, 2000.  
 Calvert, W., The detectability of ducted echoes in the magnetosphere, *J. Geophys. Res.*, **86**, 1609-1612, 1981.  
 Carpenter, D. L. and J. Lemaire, Erosion and recovery of the plasmasphere in the plasmopause region, *Space Science Reviews*, **80**, 153-179, 1997.  
 Chappell, C. R., K. K. Harris, and G. W. Sharp, A study of the influence of magnetic activity on the location of the plasmopause as measured by OGO-5, *J. Geophys. Res.*, **75**, 50-56, 1970.  
 Eastman, T. E., S. A. Boardsen, S-H. Chen, S. F. Fung, and R. L. Kessel, Configuration of high-latitude and high-altitude boundary layers, *J. Geophys. Res.*, **105**, 23221-23238, 2000.  
 Etcheto, J., G. Belmont, P. Canu, and J. G. Trotignon, Active sounder experiments on GEOS and ISEE, in Active Experiments in Space (Proc. Alpbach, Austria, 24-28 May 1983 symposium), *ESA SP-195*, 39-46, 1983.

- Fung, S. F., R. F. Benson, J. L. Green, B. W. Reinisch, D. M. Haines, I. A. Galkin, J.-L. Bougeret, R. Manning, P. H. Reiff, D. L. Gallagher, D. L. Carpenter, and W. W. L. Taylor, Observations of Magnetospheric Plasmas by the Radio Plasma Imager (RPI) on the IMAGE Mission, to be published in *Adv. Space Res.*, 2000a.
- Fung, S. F., R. F. Benson, D. L. Carpenter, B. W. Reinisch, and D. L. Gallagher, Investigations of irregularities in remote plasma regions by radio sounding: applications of the Radio Plasma Imager on IMAGE, *Space Sciences Review*, IMAGE special issue, **91**, 391-419, 2000b.
- Gallagher, D. L., and D. A. Gurnett, Auroral kilometric radiation: time-averaged source location, *J. Geophys. Res.*, **84**, 6501-6509, 1979.
- Green, J. L., D. A. Gurnett, and S. D. Shawhan, The Angular Distribution of Auroral Kilometric Radiation, *J. Geophys. Res.*, **82**, 1825, 1977.
- Green, J. L., and S. A. Boardsen, Confinement of non-thermal continuum radiation to low latitudes, *J. Geophys. Res.*, **104**, 10307-10316, 1999.
- Green, J. L., R. F. Benson, S. F. Fung, W. W. L. Taylor, S. A. Boardsen, B. W. Reinisch, D. M. Haines, K. Bibl, G. Cheney, I. A. Galkin, X. Huang, S. H. Myers, G. S. Sales, J.-L. Bougeret, R. Manning, N. Meyer-Vernet, M. Moncuquet, D. L. Carpenter, D. L. Gallagher, and P. Reiff, Radio Plasma Imager measurements, *Space Science Reviews*, IMAGE special issue, **91**, 361-389, February, 2000.
- Henize, V. K., P. H. Reiff, B. W. Reinisch, S. F. Fung, J. L. Green, J. Goldstein, Magnetospheric Cusp Observations using the IMAGE satellite Radio Plasma Imager, To be published in *Adv. Space Res.*, 2000.
- Huang, X. and B. W. Reinisch, Automatic calculation of electron density profiles from digital ionograms. 2. True height inversion of topside ionograms with the profile-fitting method, *Radio Science*, **17**, 4, 837-844, 1982.
- James, G., ISIS 1 measurements of high-frequency backscatter inside the ionosphere, *J. Geophys. Res.*, **94**, 2617-2629, 1989.
- Muldrew, D. B., Radio propagation along magnetic field-aligned sheets of ionization observed by the Alouette topside sounder, *J. Geophys. Res.*, **68**, 5355-5370, 1963.
- Morgan, D. D., and D. A. Gurnett, The source location and beaming of terrestrial continuum radiation, *J. Geophys. Res.*, **96**, 9595-9613, 1991.
- Oya, H., and T. Ono, Stimulation of plasma waves in the magnetosphere using satellite JIKIKEN (EXOS-B). Part II: Plasma density across the plasmapause, *J. Geomagn. Geoelectr.*, **39**, 591-607, 1987.
- Persoon, A. M., D. A. Gurnett, and S. D. Shawhan, Polar cap electron densities from DE 1 plasma wave observations, *J. Geophys. Res.*, **88**, 10123-10136, 1983.
- Reinisch, B. W., G. S. Sales, D. M. Haines, S. F. Fung, and W. W. L. Taylor, radio wave active Doppler imaging of space plasma structures: angle of arrival, wave polarization, and Faraday rotation measurements with RPI, *Radio Sci.*, **34**(6), 1513-1524, 1999.
- Reinisch, B. W., D. M. Haines, K. Bibl, G. Cheney, I. A. Galkin, X. Huang, S. H. Myers, G. S. Sales, R. F. Benson, S. F. Fung, J. L. Green, W. W. L. Taylor, J.-L. Bougeret, R. Manning, N. Meyer-Vernet, M. Moncuquet, D. L. Carpenter, D. L. Gallagher, and P. Reiff, The Radio Plasma Imager investigation on the IMAGE spacecraft, *Space Sciences Review*, IMAGE special issue, **91**, 319-359, February 2000.

---

B. W. Reinisch, X. Huang, D. M. Haines, and I. A. Galkin, Center for Atmospheric Research, 600 Suffolk Street, University of Massachusetts at Lowell, Lowell, MA 01854

J. L. Green, R. F. Benson, and S. F. Fung, NASA Goddard Space Flight Center, Greenbelt, MD 20771

W. W. L. Taylor, Raytheon ITSS Corporation at NASA Goddard Space Flight Center, Code 630, Greenbelt, MD

P. H. Reiff, Department of Physics and Astronomy, Box 1892, Rice University, Houston, TX 77251-1892

D. L. Gallagher, NASA Marshall Space Flight Center, Huntsville, AL 35812

J.-L. Bougeret and R. Manning, Observatoire de Paris, DESPA-URA CNRS 264, F-92195 Meudon Cedex, France

D. L. Carpenter, STAR Laboratory, Stanford University, Stanford, CA 94305

S. A. Boardsen, Emergent Information Technologies, Inc., at NASA Goddard Space Flight Center, Greenbelt, MD 20771

(Received September 26, 2000; revised December 13, 2000; accepted December 20, 2000)